Electron cyclotron heating of plasma with density above 10^{20}m^{-3} in W7-X

Yuriy TURKIN, Craig D. BEIDLER, Volker ERCKMANN, Joachim GEIGER, Heinrich P. LAQUA, Henning MAAßBERG, Nikolai B. MARUSHCHENKO, and W7-X Team

Max-Planck-Institut für Plasmaphysik, EURATOM-Association, Greifswald, Germany

12 October 2007

Electron cyclotron resonance heating (ECRH) of plasma in the Wendelstein 7-X (W7-X) stellarator at high densities is investigated by means of predictive simulations using coupled 1-D transport and ray-tracing codes. The heating efficiency and level of non-absorbed radiation are examined for various heating and plasma parameters. The transport modeling with the assumption of neoclassical core confinement has shown that high-β plasmas up to 5.5% are achievable at a magnetic field of 2.5T for the multi-pass O2-mode heating with overall absorption efficiency of 95%. The finite β-effects that can deteriorate power absorption efficiency are discussed.

Keywords: ECRH, W7-X, stellarator, plasma heating, O2-heating, steady-state operation, neoclassical transport
DOI: 10.1585

The W7-X stellarator being built at IPP-Greifswald will be equipped with a flexible ECRH system designed for 30 minutes operation with total power 10 MW generated by 10 gyrotrons [1]. The ECRH system will be the main heating source during the initial stage of W7-X operation. At low to moderate densities, heating is with the 2nd harmonic of the extraordinary mode (X2 at 140GHz and B=2.5T) with low-field-side launch in a bean-shaped plane. High-density and high-β regimes above the X2-cut-off density, i.e. from 1.2×10^{20}m^{-3} to $2\text{-}2.1\times10^{20}$m^{-3}, are accessible using the 2nd harmonic of the ordinary mode (O2).

In the present work the high performance O2-heating scenarios for W7-X are investigated by means of predictive simulations using a new 1-D transport code [2]. Neoclassical core confinement with empirical anomalous transport at the plasma edge is assumed [3]. The anomalous diffusivity scales inversely with plasma density in the region of high density gradient and exponentially decays towards the plasma axis. The radial electric field, electron and ion temperatures are advanced self-consistently with a calculation of the power deposition profiles by the ray-tracing code TRAVIS [4]. The shape of the density profile with a gradient region of about 10cm is fixed. The modeling is performed for the *standard magnetic configuration*, which is optimized for maximum confinement. More details about approaches used in simulations presented here can be found in reference [5].

Geometry of the ECRH heating system used in simulations is shown in Fig. 1. To prevent overheating of the vessel and in-vessel components by the shine-through radiation a reflecting mirror is foreseen opposite to the ECRH launchers, thus allowing the second pass absorption of the microwave beam and thereby significantly reducing the focused non-absorbed ECRH power.

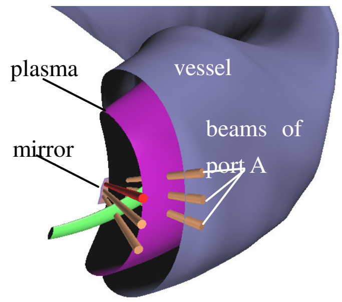

Fig. 1 Geometry of the ECRH beams; only six beams from 12 (10 plus 2 spare) [1] are shown: three beams (right) launched through port A and three beams (left) launched through port E; the other six beams are located symmetrically in the next module; the reflecting stainless-steel liners between ports are not shown. The beam in red is the spare beam.

Preliminary calculations [1] have shown that single-pass absorption of the power decreases from 80% to 50% when the density increases from 10^{20}m^{-3} to 2.1×10^{20}m^{-3} due to unfavorable temperature dependence and even after two passes of the microwave beam the non-absorbed ECRH power can be high. To increase absorption, the third pass of beams is provided by the reflecting stainless-steel liner installed on the outer side of the vessel between the ECRH ports.

author's e-mail: yuriy.turkin@ipp.mpg.de

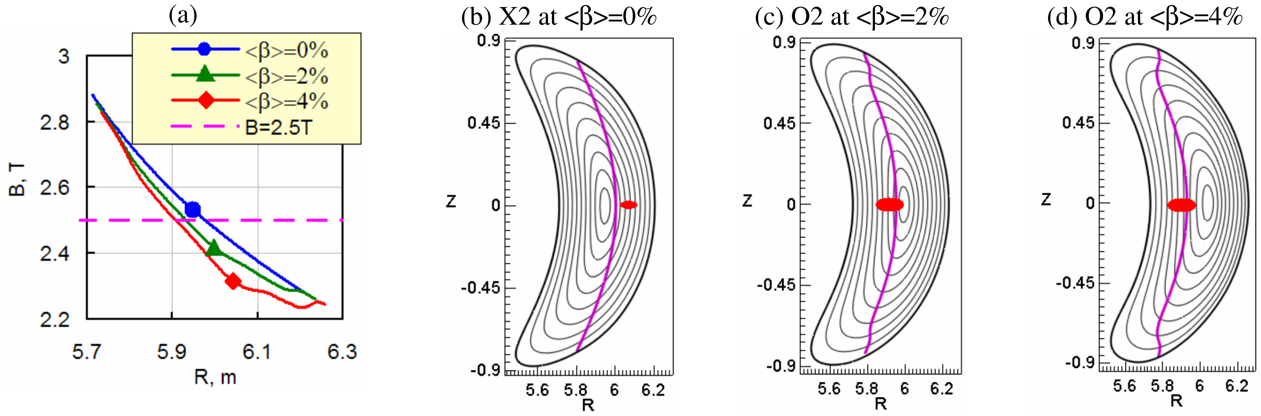

Fig. 2 Effect of high-β on the W7-X standard magnetic configuration: (a) magnetic field along major radius in bean-shape plane for different volume averaged β and the same coil currents; the magnetic axis positions are shown by markers; (b, c, d) ECRH deposition zones (red ellipses) projected onto bean-shape plane for X2/O2 heating scenarios and different magnetic configurations. The dashed line in (a) and magenta lines in (b, c, d) are the cold resonance positions (B=2.5T).

In the simulations described below all beams are aimed to the reflecting mirrors and the ray tracing code simulates three-pass absorption. The creation and sustaining of hot dense plasma by ECRH strongly depends on the magnetic field. And at the same time the high-β plasma changes the magnetic configuration. In Fig. 2a the magnetic field strength dependence on volume averaged plasma β is shown. With increasing <β> the magnetic field at the axis is reduced from 2.56T to 2.35T due to the Shafranov shift and plasma diamagnetism. Fig. 2bcd show schematically the power deposition zones which are painted by mapping of deposition profiles to the corresponding flux surfaces for the beam arrangement shown in Fig. 1. It is seen that the ECRH resonance region moves to the high field side. In this case the O2 absorption can degrade due to the decrease of the electron temperature in the resonance zone.

The ECRH power scans for the standard magnetic configuration have been performed for densities of $0.8\text{-}2.1\times10^{20}\text{m}^{-3}$ and O2-mode (140GHz at B=2.5T) heating from 1MW to 10MW taking into account the β-effects mentioned above. The value of magnetic field has been chosen to have the central O2-mode ECRH deposition for the <β>=2% configuration, see Fig. 2c. The simulations have been started from low density at given power using off-axis X2-heating (100% single-pass absorption) and vacuum magnetic configuration (Fig. 2b) with simultaneous ramp-up of the density. Then below the X2-cut-off density at $0.8\times10^{20}\text{m}^{-3}$, the magnetic configuration has been changed to the <β>=2% configuration and the polarization has been switched to O2-mode. The calculations have been continued with increasing density till O2-cut-off. To model the moving of the absorption zone from central deposition to off-axis deposition and thus absorption degradation due to the β-effects, the <β>=4% configuration (Fig. 2d) has been used for higher densities and powers; see gray areas in Fig. 3. The results of scans are depicted in Fig. 3. It is seen that nearly full absorption is achieved for a wide range of density and input power; see region below 95% curve (cyan) in Fig. 3a; the single-pass absorption for these conditions is about 70%; see Fig. 3b. The discontinuities in Fig. 3 are related to the absorption degradation for far off-axis power deposition and to the modeling procedure in which precalculated equilibriums are used instead of self-consistent recalculation of them. However the main results remain valid. In order to prevent confinement degradation, the coil currents must be raised within the range of 5% along with the β increase to compensate magnetic field decrease at the axis. The heating efficiency of the O2-mode depends on plasma parameters, especially on electron temperature, because the optical thickness is proportional to T_e^2 . The electron temperature in turn decreases with density increase as predicted by scaling laws [3] leading to absorption degradation and finally to thermal collapse; see solid red lines in Fig. 3.

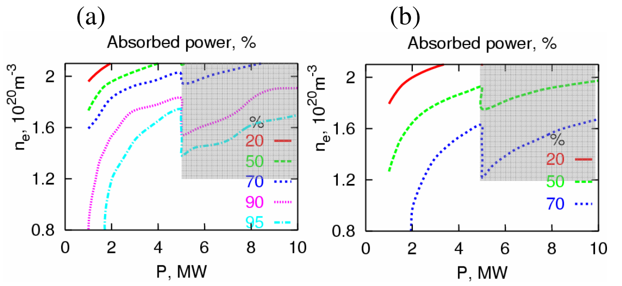

Fig. 3 Percentage of absorbed power for the three-pass scheme of O2-mode heating as a function of input power and plasma density: (a) after three passes; (b) after the first pass. Calculations in grayed area have been performed with <β>=4% equilibrium for standard magnetic configuration, for the other (n_e, P) the 2% equilibrium has been used.

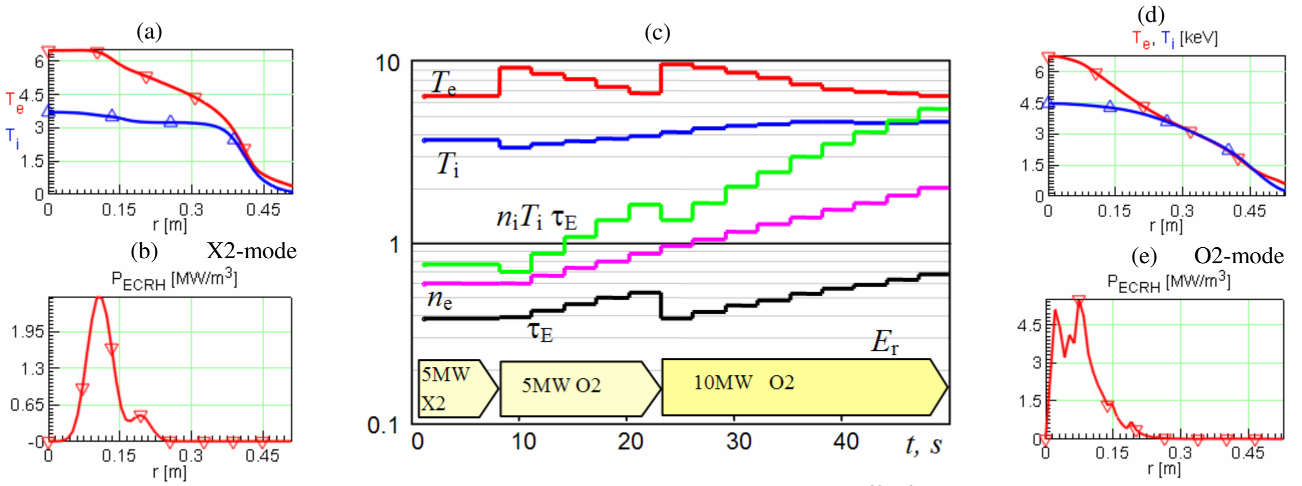

Fig. 4 (a) initial temperature and (b) low-field-side power deposition profiles at $n_e=0.6\times10^{20}m^{-3}$; (c) time evolution of the main plasma parameters: central T_e, T_i, triple product $n_iT_i\tau_E$ in $10^{20}m^{-3}$ keV·s, central n_e, energy confinement time τ_E; (d,e) final temperatures and ECRH profile at $n_e=2\times10^{20}m^{-3}$ and high-field-side deposition.

The time traces of the plasma parameters for the 10MW O2-mode scenario are shown in Fig. 4. Initially the $0.6\times10^{20}m^{-3}$ plasma is heated by 5MW X2-mode with low-field-side deposition as in Fig. 2b. Then the heating is switched to O2-mode with the same input power, but with the central deposition and $<\beta>=2\%$ magnetic configuration (Fig. 2c). The central power deposition increases the electron temperatures leading to temperature decoupling in the center. The simulation is continued by ramping-up the density (magenta curve in Fig. 4c) towards the target density $2\times10^{20}m^{-3}$. At the density $10^{20}m^{-3}$ the heating is increased to 10MW and the $<\beta>=4\%$ configuration with 5%-increase of the coil currents (that corresponds to the magnetic field increment of 0.12Tesla) to retain central power deposition is loaded. More heating increases the electron temperature; the ion temperature also goes up due to the strong collisional coupling at high densities. The final temperatures are shown in Fig. 4d, for the density profile see Fig. 6a. The following plasma parameters are reached: $n_iT_i\tau_E=5.5\times10^{20}m^{-3}$ keV·s, $\tau_E=0.67$s, and volume averaged $<\beta>=5.5\%$ with power absorption efficiency of 95%.

In Fig. 5 the projections of the beams to the poloidal and equatorial planes are shown. The intensity of red spots on the rays are proportional to the absorption rate, most of the ECRH power (>70%) is absorbed at the first pass. The beams propagate at angles optimized with respect to the absorption efficiency for O2 or X3-mode operations and refraction effects are quite small even at high density.

Finally, for comparison with O2 ECRH plasmas, we have simulated the plasma heated by "positive" NBI (p-NBI, 60 keV H^+); see Fig.6. In the p-NBI case, the main power is absorbed at outer radii, especially the low energy components of the beam. This leads to confinement degradation, whereas for the O2 case the more central

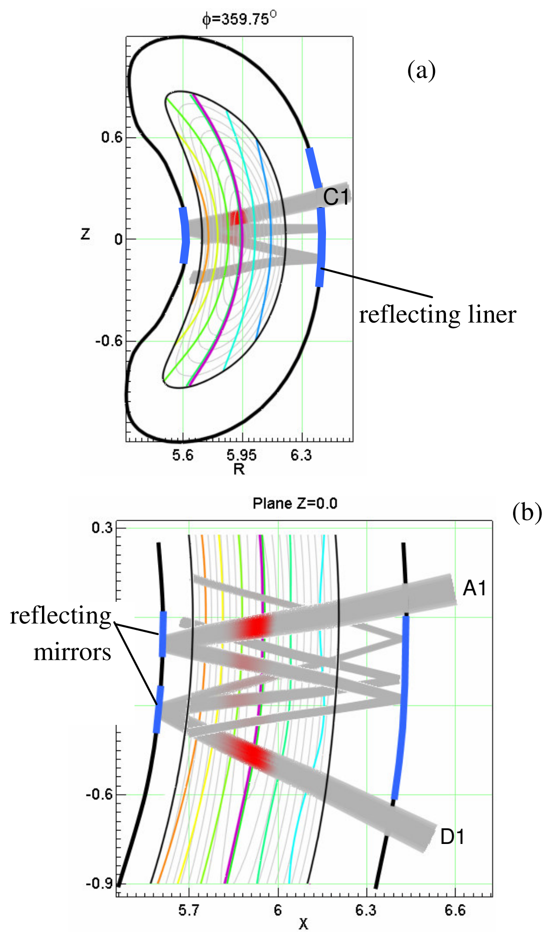

Fig. 5 Trajectories of ECRH beams: (a) poloidal plane with only one beam shown, (b) equatorial plane with the two beams going from mirror A1 of port E and mirror D1 of port A; magenta lines are the cold resonance positions; color lines in figures are the lines of constant magnetic field.

deposition allows for higher temperatures and improved confinement times. Indeed for these heating parameters, τ_E=0.46s at <β>=4.2% and τ_E=0.67s at <β>=5.5% are obtained for p-NBI and O2 ECRH, respectively.

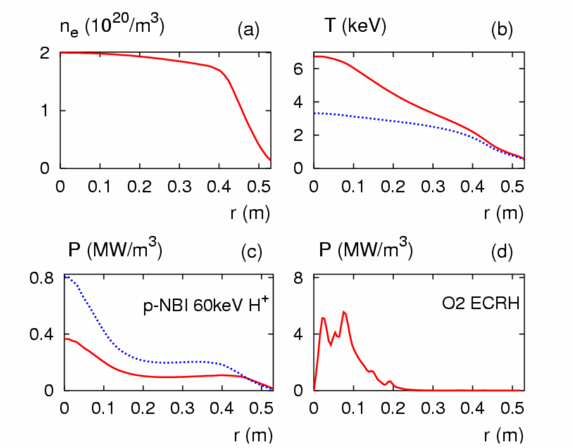

Fig. 6 (a) and (b): Plasma profiles for a 10MW heating simulation of W7-X. The solid line in figure (b) refers to O2 ECRH power depositions in plot (d). The dotted line in (b) refers to NBI power depositions shown in plot (c). The dotted line in (c) corresponds to the power deposited to ions.

Summary

The O2-ECR heating efficiency is analyzed for various plasma parameters and heating conditions using ray tracing modeling coupled with a 1D-transport code. The transport modeling with the assumption of neoclassical core confinement has shown that high-β plasmas up to 5.5% are achievable at a magnetic field of 2.5T for the multi-pass O2-mode heating with overall absorption efficiency of 95%. The O2-mode heating scenarios look promising for high-density-operation regimes of W7-X with high separatrix density that is the most favorable condition for operation of the divertor. It is worth noting that the neoclassical predictions give an upper limit of plasma performance in W7-X. Further predictive transport simulations will be considered for high-β plasmas for which the moving of the resonance zone due to the Shafranov shift and the diamagnetic current can decrease absorption efficiency.

[1] V. Erckmann, P. Brand et al. Electron cyclotron heating for W7-X: Physics and Technology**.** *Fusion science and technology***,** 52, 291(2007)

[2] Yu. Turkin, H. Maaßberg et al. *Fusion Science and Technology*, **50**, 387(2006)

[3] Yu. Turkin, C. D. Beidler et al. Transport Simulations for W7-X. *33rd EPS Conference on Plasma Phys.* Rome, 19 - 23 June 2006 ECA Vol.30I, P-2.113 (2006)

[4] N. B. Marushchenko et al. in *Proc. of the 16th Toki Conf.*, Japan, December 2006, http://itc.nifs.ac.jp/index.html

[5] C. D. Beidler, J. Geiger et al. Transport Modeling for W7-X on the Basis of W7-AS Experimental Results. Paper I-21 in *Proc. of the 17th Toki Conf.*, Japan, October 2007